Article

Exploring Olive Pit Powder as a Filler for Enhanced Thermal Insulation in Epoxy Mortars to Increase Sustainability in Building Construction

Veronica D'Eusanio [1,2,*], Andrea Marchetti [1,2,3], Stefano Pastorelli [4], Michele Silvestri [4], Lucia Bertacchini [4] and Lorenzo Tassi [1,2,3]

1 Department of Chemical and Geological Sciences, University of Modena and Reggio Emilia, 41121 Modena, Italy; andrea.marchetti@unimore.it (A.M.); lorenzo.tassi@unimore.it (L.T.)
2 National Interuniversity Consortium of Materials Science and Technology (INSTM), 50121 Florence, Italy
3 Interdepartmental Research Center BIOGEST-SITEIA, University of Modena and Reggio Emilia, 42121 Reggio Emilia, Italy
4 Litokol S.p.A. Research Center, 42048 Rubiera, Italy; stefano.pastorelli@litokol.it (S.P.); michele.silvestri@litokol.it (M.S.); lucia.bertacchini@litokol.it (L.B.)
* Correspondence: veronica.deusanio@unimore.it

Abstract: This article explores the use of olive pit powder (OPP) as a promising resource for enhancing the thermal insulation properties of epoxy mortars. A comprehensive analysis of the chemical and physical characteristics of OPP was conducted, employing analytical techniques including scanning electron microscopy (SEM), thermogravimetric analysis and emitted gas analysis (TG-MS-EGA), and proximal analysis. Experimental samples of epoxy grout were prepared by using different proportions of a conventional inorganic filler, quartz powder, and OPP within an epoxy mortar matrix. As the percentage of OPP in the formulation increased, the microstructure of the samples gradually became more porous and less compact. Consequently, there was a decrease in density with the increase in OPP content. The 28-day compressive strength decreased from 46 MPa to 12.8 MPa, respectively, in the samples containing only quartz (Sample E) and only OPP (Sample A) as a filler. Similarly, flexural strength decreased from 35.2 to 5.3 MPa. The thermal conductivity decreased from 0.3 W/mK in Sample E to 0.11 in Sample A. Therefore, increasing the %wt of OPP improved insulating properties while reducing the mechanical resistance values. This study highlights the potential of OPP as an environmentally friendly and thermally efficient filler for epoxy mortars, thereby promoting sustainable construction practices.

Keywords: sustainability; olive pit powder; building construction; epoxy mortars; thermal conductivity

1. Introduction

Epoxy mortars are widely employed in construction owing to their rapid curing process, high compressive strength, strong adhesion capabilities, very low permeability, and remarkable chemical resistance [1–5]. Their potential extends to various construction needs requiring durable solutions. For instance, industrial flooring benefits from the robust properties of epoxy composites, ensuring longevity and resilience against heavy machinery and high foot traffic, which are critical aspects in many manufacturing environments. Furthermore, the production of railway sleepers, which are essential components of railway infrastructure, benefits in terms of increased durability and longevity owing to the use of epoxy materials. The widespread adoption of epoxy composites faces a significant barrier due to the high costs associated with epoxy resins, particularly when compared to conventional Portland cement [6,7]. This cost disparity can be attributed to several factors, including the intricate manufacturing processes involved in producing high-quality epoxy resins and the raw materials required for their formulation.

Epoxy resins are prepolymers characterized by an epoxy group at each end of their molecular structure. Among the widely used options, Bisphenol A diglycidyl ether (DGEBA) is the most prevalent. Hardeners, also referred to as curing or crosslinking agents, act by opening the C–O–C ring at the ends of an epoxy molecule, attaching to them, and transforming the resin into a thermosetting network. Amino-type hardeners are the most used choice for epoxy resins. Inorganic fillers, such as silica, quartz, $CaCO_3$, and alumina, serve as integral components in epoxy mortars by imparting mechanical strength and dimensional stability. Reactive diluents are designed to reduce the viscosity of conventional epoxy resins while preserving their essential performance characteristics. These diluents, which are mono- or di-functional compounds, include aliphatic and aromatic glycidyl ethers that covalently bond to the polymer matrix. This linkage ensures the firm integration of reactive diluents within the resin structure, thereby preventing any propensity for migration.

Sustainable development involves efficient use of natural resources and the progression of innovative ecological technologies. This pursuit includes various strategies, such as the reduction of polluting emissions, the conscious consumption of raw materials, and a heightened focus on waste recycling. Pursuing sustainable development in the production of building materials involves the incorporation of waste and recyclable materials [8,9], since the extraction and processing of virgin resources can be environmentally destructive and energy-intensive [10,11]. This can lead to habitat loss, air and water pollution, and depletion of natural resources. This concept forms the basis of the scientific exploration presented in this study, which explores the innovative application of olive pit powder as a sustainable alternative to traditional inorganic fillers in epoxy mortars. Olive pit powder, a finely ground residue derived from olive processing, is an abundant and widely available waste material, particularly in countries with significant olive oil production, such as Italy, Greece, Spain, and other Mediterranean regions. This repurposing of waste material aligns with principles of circular economy, minimizing environmental impact and reducing reliance on virgin resources. Various waste materials have been incorporated into epoxy resins to reduce the demand for natural resources and to improve their mechanical properties. Previous studies have included fillers, such as silica fume [12], red mud [13,14], sand washing wastes [6], coal bottom ash [7,15], fly ash [12,16], blast furnace slag [17], and palm oil fuel ash [18]. In some cases, industrial waste materials exhibit distinctive properties that make them suitable for specific applications. Specifically, bio-aggregates such as oil palm shells, coconut shells, bamboo, and apricot shells represent promising options for enhancing thermal insulation and sound absorption in cement-based building materials [19,20]. The thermal insulation property is of fundamental importance in the current global context, in which energy consumption has grown together with the global economy and urban and industrial activities [21,22]. Building energy conservation plays a crucial role in mitigating energy consumption, and thermal insulation materials hold a significant value in the realm of building energy conservation [23–26]. Bio-based lightweight aggregates typically consist of carbohydrate structures and exhibit high porosity. This high porosity can be advantageous for thermal insulation, as air, being a poor conductor of heat, fills the voids within the aggregates. When lightweight aggregates contain numerous air pockets due to their porosity, the overall thermal conductivity of the mortar is reduced. This creates a barrier that hinders heat transfer, making the material a better thermal insulator. Despite this advantage, some bio-aggregates can be susceptible to moisture absorption due to their porous nature. When exposed to environmental humidity fluctuations, this moisture absorption can compromise the durability of cement-based materials. However, when it comes to epoxy-based building materials, a more favorable scenario unfolds in terms of durability, owing to their intrinsic resistance to weathering. Consequently, the use of durable epoxy-based mortars in combination with bio-based aggregates can offer enhanced longevity and resilience to construction materials, overcome the challenges posed by environmental humidity, and ensure sustainable and robust building solutions. The integration of such an environmentally conscious filler, olive pit powder, not only addresses

the issue of waste management, but also represents an exploratory study with the aim of increasing the thermal insulation properties of epoxy-based materials. To the best of our knowledge, this study represents the first systematic exploration of using olive pit powder as a filler in epoxy mortars. The use of this eco-friendly filler can open new possibilities for the use of epoxy mortars in sustainable and energy-efficient applications, coupling the insulating power of olive pit powder with the durability of epoxy binders. For example, considering that coating mortar serves as the building envelope and its thermal properties help to reduce energy consumption, incorporating lightweight materials with favorable thermal characteristics can enhance the thermal comfort of mortars in addition to reducing the overall weight of buildings [27].

In this study, five formulations of epoxy mortars were prepared and characterized, incorporating percentages of olive pit powder as a replacement for a common inorganic filler, namely quartz powder. This comparative analysis was undertaken to investigate the influence of olive pit powder content on the physiochemical properties of the epoxy mortar formulated with quartz powder, selected as a reference because of its widespread commercial availability and common usage. The properties of density, compressive and flexural strengths, and thermal conductivity were evaluated. Additionally, insights into the microstructures of the epoxy mortars were obtained via SEM analysis. Furthermore, this study examined the olive pit powder filler by conducting a proximate analysis and characterizing it through TG-MS-EGA analysis and microscopic analysis via SEM. Single types of epoxy resin, reactive diluent, and hardener were chosen for examination. The most commonly used DGEBA epoxy resin was used in this study. Owing to the high resin absorption capacity of olive powder, it was necessary to add varying amounts of reactive diluent to achieve good workability of the mixture. Therefore, a low-viscosity reactive diluent was chosen to counteract the viscosity increase resulting from the addition of the olive pit powder.

2. Materials and Methods

2.1. Fillers

In this study, olive pit powder (OPP) was used as filler to replace quartz in different proportions. OPP was sourced from BioPowder (Schilling Ltd., Birkirkara, Malta; https://www.bio-powder.com/en/olive-pit/, accessed on 12 December 2023). The particle size was 100–300 μm. The quartz sand, with particle sizes ranging between 150 and 300 μm, had a purity of 95%.

2.2. Epoxy Resin, Hardener, and Reactive Diluent

Diglycidyl ether of Bisphenol A-type epoxy resin (DGEBA) was used in the proportion mixture as shown in Table 1. The epoxy resin was stored at room temperature to avoid damage. An aliphatic hardener, trimethyl hexamethylene diamine (TMDA), was used. A monofunctional reactive diluent (glycidylether C12-C14 alcohol, RDMF) was employed as the reactive diluent. The proprieties of the selected epoxy resin, hardener, and reactive diluent are reported in Table 1.

Table 1. Properties of the epoxy resin, hardener, and reactive diluent used.

	Density (g/mL)	Viscosity (cp.)	Epoxy Equivalent Weight (g/val)	Molecular Weight (g/mol)
DGEBA	1.16	16,600	195.1	-
TMDA	0.88	6	-	158.4
RDMF	0.87	10	289.5	-

2.3. Mix Proportions

The mix proportions (% weight) of the epoxy mortars are given in Table 2. The mixing proportions of epoxy resin/hardener/filler were consistently maintained at a ratio of 1:0.4:3.45. Variations in the content of the reactive diluent were introduced to ensure the

optimal workability of the mixture, achieved by regulating its viscosity. This adjustment in the reactive diluent content was made to strike a balance, ensuring that the mixture remained manageable and suitable for application while maintaining the specified overall composition of the epoxy system.

Table 2. Composition of the studied epoxy grouts.

Grouts	Epoxy Resin %	Hardener %	Reactive Diluent %	OPP %	Quartz Powder %
A	18.5	7.4	10.4	63.7	0
B	18.7	7.5	9.2	48.4	16.2
C	19.0	7.6	8.0	32.7	32.7
D	19.2	7.7	6.8	16.6	49.7
E	19.5	7.8	5.5	0	67.2

2.4. Specimen Preparation

The specimens were prepared following a systematic procedure: OPP, quartz powder, and epoxy resin were combined in a blender and homogenously mixed for a duration of 10 min. Subsequently, the mixture was allowed to stand for 24 h in a dark environment. The hardener was introduced and stirred for an additional 5 min. Following this mixing process, the freshly prepared mixtures were poured into prismatic molds (40 mm × 40 mm × 160 mm) and compacted using a vibrating table for 30 s. The specimens were then positioned in a controlled environmental chamber at 20 °C and 50% RH, and removed from the molds after an approximate curing period of 24 h. The curing of the specimen was performed for 28 more days in the same condition. Six specimens were prepared for each formulation: three for the analysis of flexural and compressive strength, as described in Section 2.6.1, and three for the thermal conductivity analysis. The dimensions of the specimens follow the European standard for grouts and adhesives (EN 13888-ISO 13007 [28,29]).

2.5. Characterization of OPP

2.5.1. Proximate Composition

Moisture, ash, crude protein, and residual oil were assessed in accordance with protocols recommended by the Association of Official Analytical Chemists. Moisture content was determined by drying the OPP sample at 105 °C until a constant weight was achieved. Ash content was quantified utilizing a laboratory furnace at 550 °C, with a gradual temperature ramp. Nitrogen content, determined via the Dumas method, was subsequently converted to protein content using a conversion factor of 6.25. The Soxhlet method, employing petroleum ether (boiling point range: 40–60 °C) as the extractant solvent, was applied to determine the residual fat fraction. Each measurement was performed in triplicate, and the results were averaged.

2.5.2. Particle Size Distribution

The particle size distribution was measured through the laser diffraction technique by using Mastersizer 3000 (Malvern Panalytical Ltd., Malvern, UK). The measurements were conducted in an aqueous environment. The samples were pre-dispersed in water in order to accomplish better dispersion of the particles.

2.5.3. SEM

The field emission scanning electron microscope (SEM) instrument (Nova NanoSEM 450, FEI, Hillsboro, OR, USA) was used to evaluate the microscopic morphology of the OPP filler.

2.5.4. TG-MS-EGA

The thermogravimetric analysis (TGA) was conducted using a Seiko SSC 5200 thermal analyzer (Seiko Instruments Inc., Chiba, Japan) within an inert atmosphere. Gas analysis of the evolved products during thermal reactions (MS-EGA) was performed employing a coupled quadruple mass spectrometer (ESS, GeneSys Quadstar 422; ESS Ltd., Cheshire, UK). Sampling procedures utilized an inert and fused silicon capillary system, preheated to prevent condensation.

Signal intensities of specific target gases were acquired in multiple ion detection mode (MID) through a secondary electron multiplier operating at 900 V. Specifically, m/z ratios of 18 for H_2O, 44 for CO_2, 60 for $C_2H_4O_2$ (acetic acid), and 30 for $C_3H_3^+$ (furfural fragment) were selected, with m/z representing the ratio between the mass number and the charge of the ion.

The heating protocol involved a gradient of 20 °C/min over the thermal range of 25–1000 °C, utilizing ultrapure helium as the purging gas at a flow rate of 100 µL/min.

2.6. Properties of the Epoxy Mortars

2.6.1. Flexural and compressive strength

Flexural and compressive strength testing was performed after 28 days using a Technotest compression test machine (Technotest, Modena, Italy). The average value of at least three specimens was used as the test result. The test was performed in conformity with the European standard for grouts and adhesives (EN 13888-ISO 13007 [28,29]). Three-point flexural testing was conducted to determine the flexural strength of the specimens followed by a compressive strength test using the remaining broken pieces from the flexural tests, at a loading rate of 800 N/min.

2.6.2. Thermal Conductivity

A KD2 Pro thermal property analyzer (Decagon Inc., Pullman, WA, USA) was employed for measuring thermal conductivity. This portable device fully adheres to ASTM D5334-08 standards [30] and is designed for assessing the thermal properties of materials using probe/sensor methods (transient line heat source), as confirmed by the Decagon Devices Inc. Operator Manual version 11. The analyzer comprises a portable controller and a sensor probe that is inserted into the medium being measured. The measurement procedure involves heating the probe for a specified duration while monitoring the temperature during both the heating and cooling phases. It is crucial to minimize the influence of ambient temperature on the samples to obtain more precise values. The KD2 Pro has a measurement range for thermal conductivity ranging from 0.02 to 2.00 W/mK. In this study, three cubic specimens were selected for each sample, measuring 100 mm × 100 mm × 100 mm, and were assessed at 28 days of curing under dry conditions to determine thermal conductivity.

3. Results and Discussion

3.1. Olive Pit Powder

3.1.1. Proximate Composition of Olive Pit Powder

Table 3 provides the proximate composition of olive pit powder (Figure 1), the vegetable filler used in this study, offering a detailed overview of its chemical composition. Data are expressed as the mean ± standard deviation of three replicates.

Analyzing the proximate composition of raw materials is important for assessing their potential applications across various industrial sectors. Proximate analysis of vegetable materials involves determining fundamental chemical components, such as moisture, ash, fat, protein, cellulose, hemicelluloses, and lignin [31]. Moisture content is a critical parameter that affects the stability, shelf life, and processing characteristics of a material. Microorganisms such as bacteria and fungi require moisture to thrive [32]. The low moisture content in OPP (3.4%) ensures conditions less favorable to microbial growth. This inhibits the development of spoilage and degradation, contributing to the preservation of the material over time. It is important to maintain these moisture levels, as one of the main challenges in

the industrial utilization of organic materials is degradation over time if not stored properly. Factors such as exposure to moisture, temperature fluctuations, and prolonged storage periods can degrade the quality of olive pit powder, potentially impacting its performance. Ensuring proper storage conditions and implementing effective preservation techniques are essential to mitigate these challenges and maximize the usability and effectiveness of olive pit powder in industrial applications. The matrix exhibits a typical composition of woody biomasses, characterized by a low protein content (<3%) and a cellulose, hemicellulose, and lignin content exceeding 80% on a dry basis. The lipid percentage is slightly higher than that of other woody matrices [19,33,34], which is not surprising given the high lipid content in the olive fruit. This composition aligns with the inherent characteristics of olive pit biomass, highlighting its lignocellulosic nature and the influence of lipid-rich olive fruits on the overall matrix composition.

Table 3. Proximate composition of olive pit powder. Data are expressed as mean $\pm$ standard deviation.

|	
Moisture (%)	3.4 ± 0.6
Cellulose (%)	36.0 ± 0.7
Hemicelluloses (%)	26.3 ± 0.6
Lignin (%)	24.6 ± 0.9
Protein (%)	2.3 ± 0.5
Fat (%)	5.0 ± 0.9
Ash (%)	2.4 ± 0.7
C (%)	51.7 ± 0.4
O (%)	41.0 ± 0.5
N (%)	0.37 ± 0.06
H (%)	7.12 ± 0.19
S (%)	<0.1
Bulk density (g/cm^3)	0.508 ± 0.008

Figure 1. The vegetable filler used in this study: olive pit powder.

3.1.2. Particle Size Distribution

To assess the particle size distribution of the olive pit powder, a laser diffraction technique was employed, and the results are shown in Figure 2. The analysis revealed that the OPP exhibited a mean particle diameter of approximately 400 μm. The distribution profile indicates a predominantly uniform size range with minimal variance in particle

dimensions. This consistent particle size distribution is of particular significance for applications in epoxy mortars because it suggests a homogenous blending potential with the matrix material.
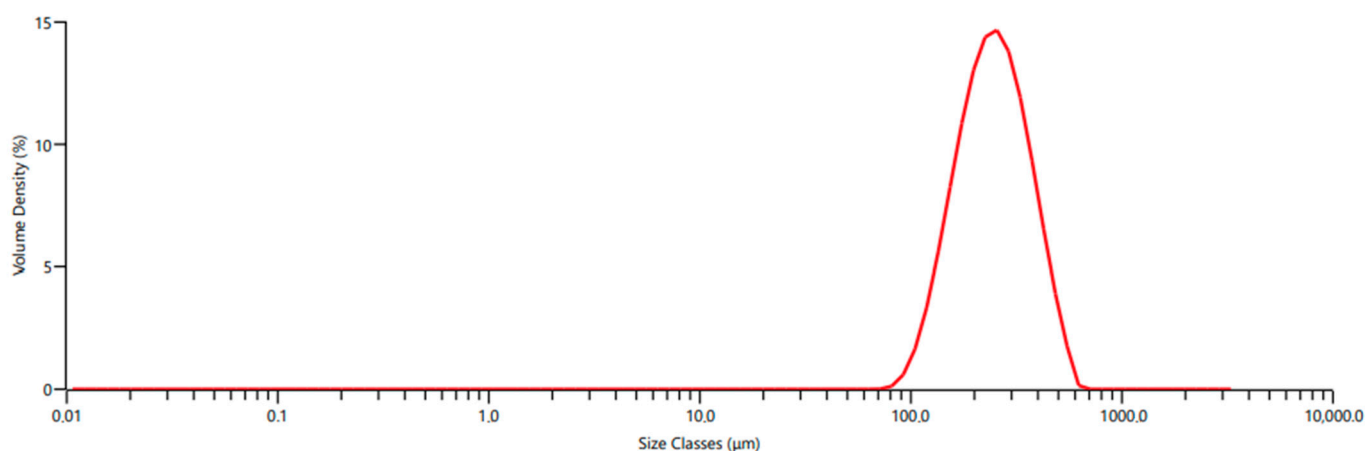
Figure 2. Particle size distribution of olive pit powder.

3.1.3. SEM Analysis

The SEM images in Figure 3A,B provide a detailed view of the surface morphology of olive pit powder granules. The surfaces exhibited a distinct rough texture characterized by irregularities and a lack of discernible cavities. The granules had a densely packed structure, suggesting a high degree of particle cohesion. They appear pseudospherical, a morphology consistent with the typical effect of fluidized bed grinding in a stream of compressed air. This morphological analysis underscores the potential suitability of olive pit powder as a filler material in epoxy mortars because the observed surface characteristics may enhance interfacial adhesion and contribute to the overall mechanical properties of the composite material. The absence of prominent voids or irregularities further suggests a uniform and potentially reinforcing distribution of the olive pit powder within the epoxy matrix.

3.1.4. TG-MS-EGA

Olive pit powder is predominantly composed of lignocellulosic material, comprising cellulose, hemicellulose, and lignin, as indicated in Table 2. Through thermogravimetric analysis coupled with mass spectrometry and evolved gas analysis (TG-MS-EGA), we gained valuable insights into the intricate degradation processes involving all constituents present in OPP and into the pyrolytic behavior of the biomass. This analytical technique allows us to discern distinct thermal ranges within the thermogram, each corresponding to specific degradation events.

Given the complex composition of olive pit powder, which is characterized by multiple organic components, different degradative reactions can occur concurrently. Consequently, the resulting thermogram profile represents a composite of these diverse contributions. However, interpreting individual degradation processes from thermograms can be challenging, particularly when different reactions produce similar byproducts, such as water and carbon dioxide.

To facilitate the interpretation of the thermogram, the entire temperature range was divided into thermal regions of varying sizes and characteristics, as shown in Figure 4. Additionally, Table 4 provides insight into the specific thermal windows or subdomains within these regions, where distinctive deviations in the TG/DTG profiles are observed. These deviations correspond to the unique behaviors exhibited by the studied samples during degradation.

(A)

(B)
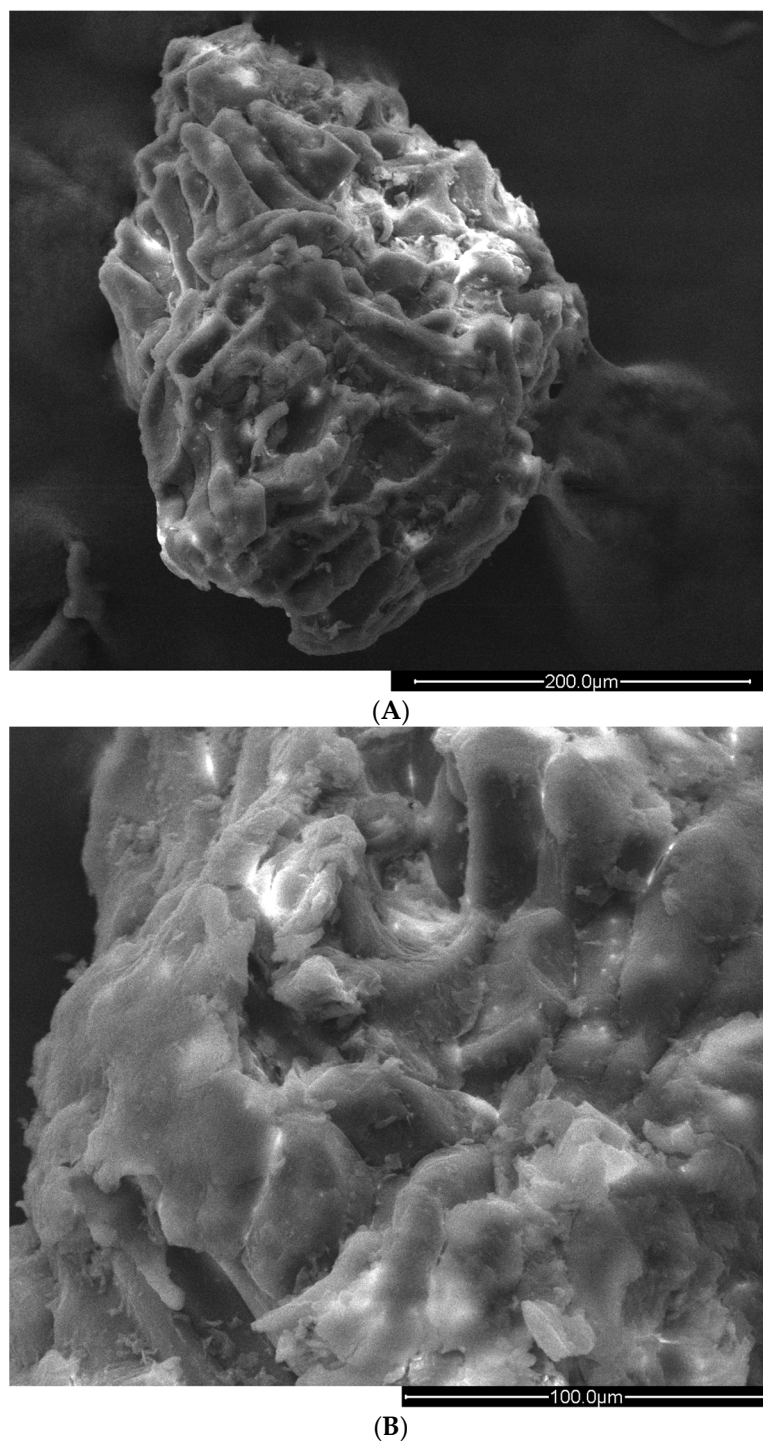
Figure 3. (**A**) Olive pit powder granule at 600× magnification. (**B**) Olive pit powder granule at 300× magnification.

The TGA curves show that the devolatilization process starts at 40 °C and the maximum weight loss occurs in the range of 220–400 °C. Above 400 °C, after the change in the slope of the TGA, a slower weight loss occurs. The evaluation of the weight loss of the samples between 120 °C, the end of moisture evaporation, and 400 °C indicates that more than 70 wt% of the volatile matter was released in this interval.

Table 3 shows that approximately 87% of the olive pit powder (OPP) consists of cellulose, hemicellulose, and lignin. Thus, the TG-MS-EGA analysis delineated the thermal degradation steps associated with these three fractions. Consequently, the evolution of

select analytes characteristic of hemicellulose and cellulose degradation, such as acetic acid (m/z = 45 and 43 for its main fragments) and furfural (m/z = 39 for its fragment $C_3H_3^+$), was examined through mass spectrometry–evolved gas analysis (MS-EGA). This comprehensive analysis enables a more precise differentiation of the thermal processes and identification of the temperature ranges corresponding to each matrix component. The evolutionary trends of the selected gaseous species are shown in Figure 5.
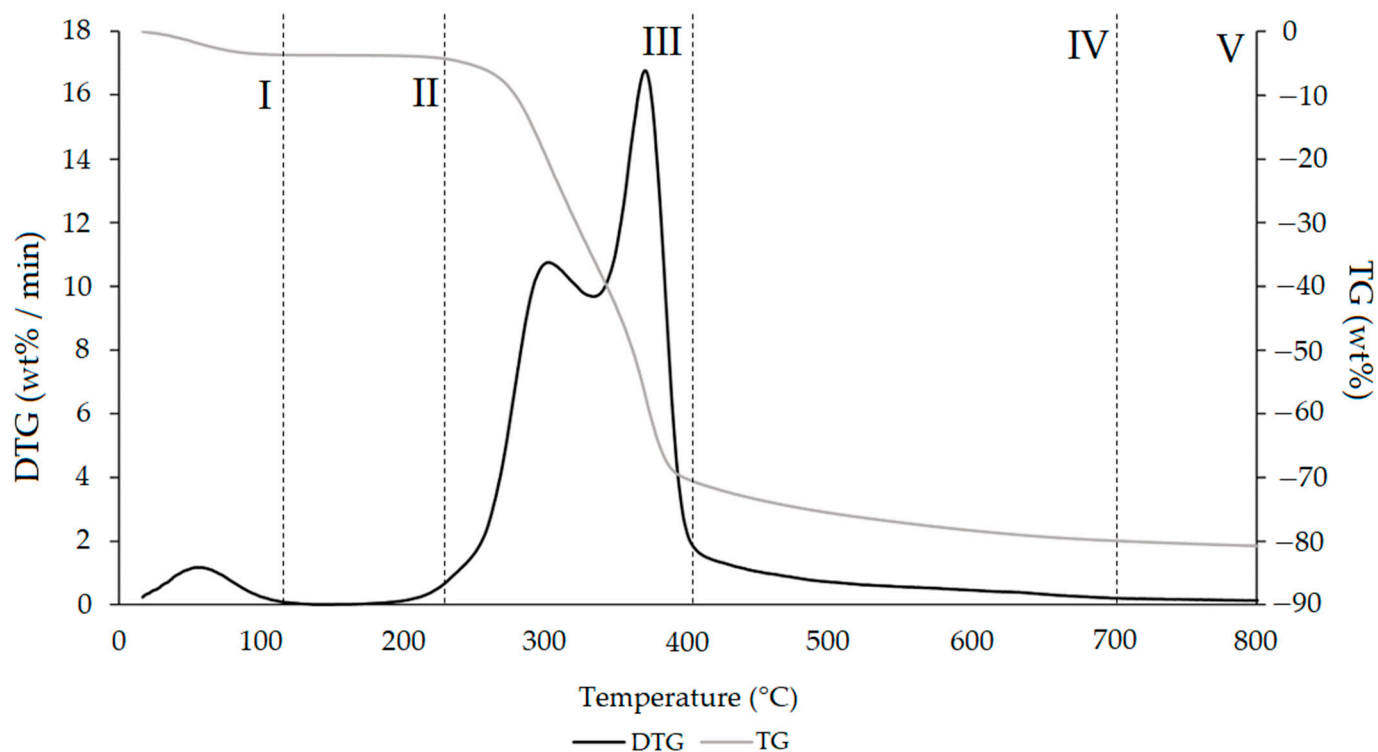
Figure 4. TG (gray line) and DTG (black line) curves of OPP sample at heating rate of 20 °C/min in He atmosphere. Vertical dashed lines delimit the five thermal regions (I–V) described in the text. For the meaning of the number in parentheses, see Table 3.

Table 4. Thermal degradation regions and processes of olive pit powder biomass identified through thermogravimetric analysis (TG).

Region	Thermal Window	Thermally Activated Processes	Mass Loss ($-\Delta m$ %)
I	Up to ~120 °C	Removal of moisture and VOCs.	−3.7
II	120–210	Removal of bound water, NH_3 from free amino acids and protein denaturation, low-boiling VOCs, and loss of CO and CO_2.	−0.3
III	210–415	Removal of reaction water, high-boiling VOCs and SVOCs, decarboxylation of acids with CO_2 loss, and fat degradation. Main pyrolysis window, structural decay reactions of proteins, hemicellulose, and cellulose.	−67.5
IV	415–700	Removal of reaction water, CO_2, and CO from slow pyrolysis of lignin fraction, vitrification of sample, volatilization of carbon microparticles, and thermal decomposition of biochar.	−8.5
V	700–800	Volatilization of carbon residues, probably C20–C40 fragments, in the presence of mineral ash.	−0.8
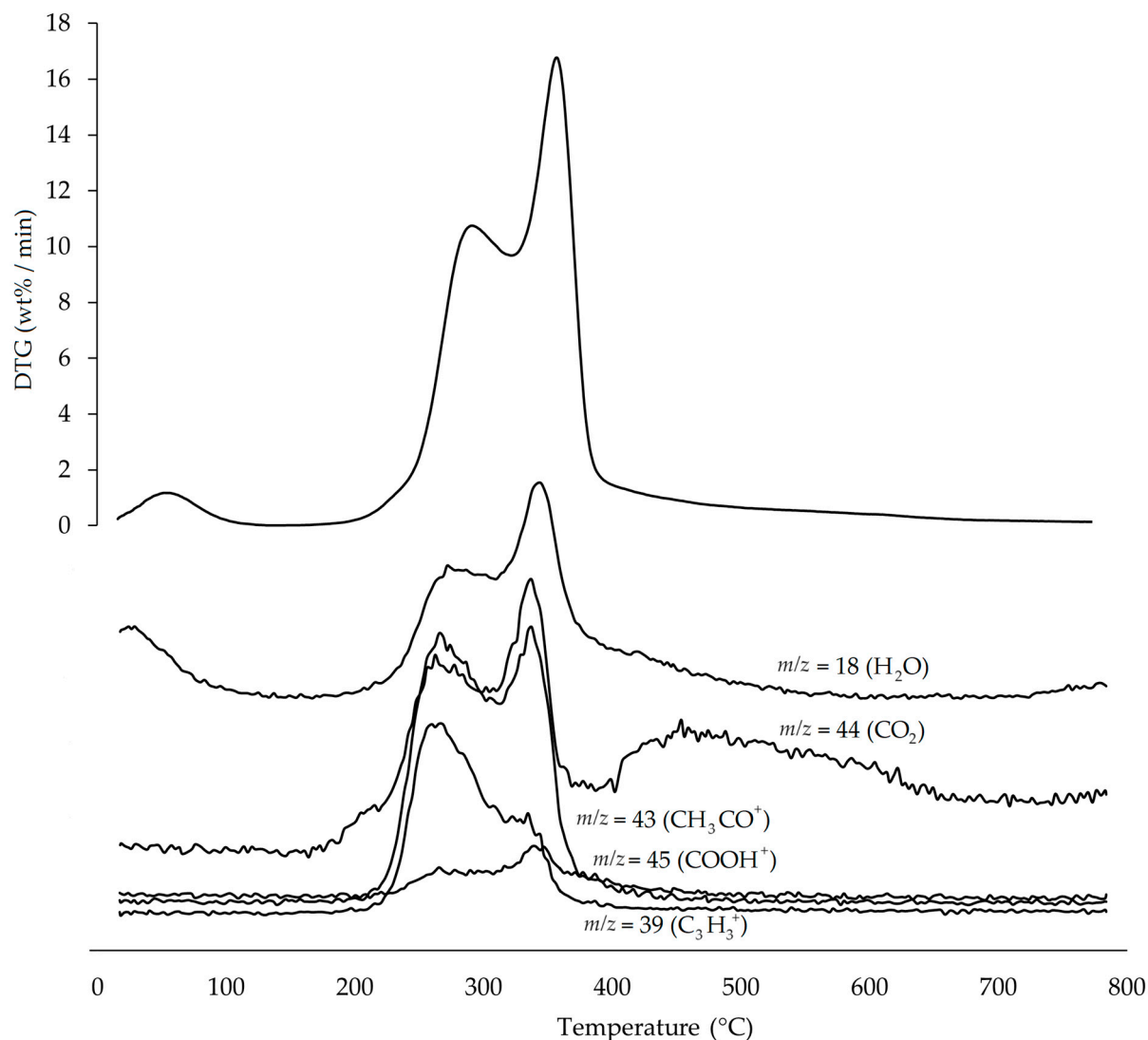
Figure 5. Evolutionary trends of H_2O, CO_2, furfural fragment ($C_3H_3^+$, $m/z = 39$), and acetic acid fragments (CH_3CO^+, $m/z = 43$; $COOH^+$, $m/z = 45$) during the heating of the OPP sample. The derivative thermogravimetric (DTG) curve is also displayed for ease of comparison. Intensity of m/z is in arbitrary units.

The thermograms are divided into five distinct regions (I–V), each representing the behavior of the sample in response to specific processes. The limits defining these regions are not strictly fixed at absolute temperature values. Instead, they represent dynamic thresholds influenced by thermally activated processes that are specific to material fractions. Attempting to generalize the thermal intervals for each region could lead to speculative conclusions, in contrast to the rigorous methodology adopted in this study.

Region I, spanning up to ~120 °C, primarily involves the removal of moisture and volatile organic compounds (VOCs) [35]. Additionally, thermally activated processes such as protein denaturation by unfolding occur within this region without accompanying mass loss.

Region II, ranging from ~120 °C to ~210 °C, corresponds to the loss of bound water, including the crystallization of mineral salt water. Here, semi-volatile compounds with medium-low vapor pressure (SVOCs) are fully eliminated. The initiation of structural water removal at 160 °C involves the condensation reactions of −OH groups, which are primarily present in simple non-cellulosic carbohydrates [36]. Furthermore, the evolution and removal of reaction water span this entire thermal range up to region IV. Near the

upper-temperature limit (~180 °C), thermal degradation of free amino acids occurs [37], while proteins persist up to ~200–220 °C, signifying the onset of biomass chemical structure destabilization, partial depolymerization, and plasticization.

Region III, spanning from ~210 °C to ~415 °C, constitutes the principal pyrolysis window, where structural decay reactions of proteins (~240 °C), hemicellulose (250–300 °C), cellulose (300–380 °C), and lignin (300–500 °C) occur. The emission of acetic acid and furfural in this thermal window confirmed the thermal degradation of cellulose and hemicellulose, as reported in previous studies [38,39]. In particular, acetic acid formation is related to the elimination of O-acetyl groups linked to the main xylan chain, while furfural formation is linked to the dehydroxymethylation of the furan ring side chain in 5-hydroxymethylfurfural, an organic compound formed by the dehydration of reducing sugars [38,39]. The shape of the peaks is determined by the constituent that degrades within the specific thermal window [40]. Indeed, the amorphous structure of hemicellulose results in a broad peak in the 250–300 °C range, whereas the high homogeneity and crystallinity of the cellulose polymer lead to a sharp peak at 300–350 °C. Lignin, due to its structural complexity, degrades over a broad temperature range, and its degradation pattern varies significantly due to its compositional variability [41,42].

Region IV begins at approximately 415 °C and extends to approximately 700 °C. Within this thermal window, the gradual decrease in mass primarily arises from the slow pyrolysis of the lignin fraction, a process associated with sample vitrification and volatilization of carbon microparticles. The minor mass loss up to 700 °C can also be attributed to the thermal decomposition of carbonaceous matter (biochar), which is predominantly associated with hemicellulose and cellulose fractions [43,44]. In this thermal range, the emission mainly of CO_2 is observed (Figure 5).

In region V, above approximately 700 °C and up to the final temperature of 800 °C, the remaining residues of biomass degradation are observed. This represents the typical carbon pyrolysis window, characterized by the thermal decomposition of low volatile matter such as carbon fragments C20–C40 in the presence of mineral ash.

The TG/DTG profiles of the olive pit powder (OPP) exhibit characteristics typical of lignocellulosic raw materials, underscoring the presence of hemicellulose, cellulose, and lignin. This observation is further corroborated by proximate composition analysis (refer to Section 3.1.1 and Table 2).

3.2. Epoxy Resin Mortar

The cross-sections of five representative samples from the five epoxy mortar formulations are shown in Figure 6. A trend emerges as the percentage of OPP increases: the internal structure of the samples undergoes a morphological change, characterized by an increase in the presence of pores and cavities. This macroscopic observation is further validated in Section 3.2.1 through scanning electron microscope (SEM) analysis.
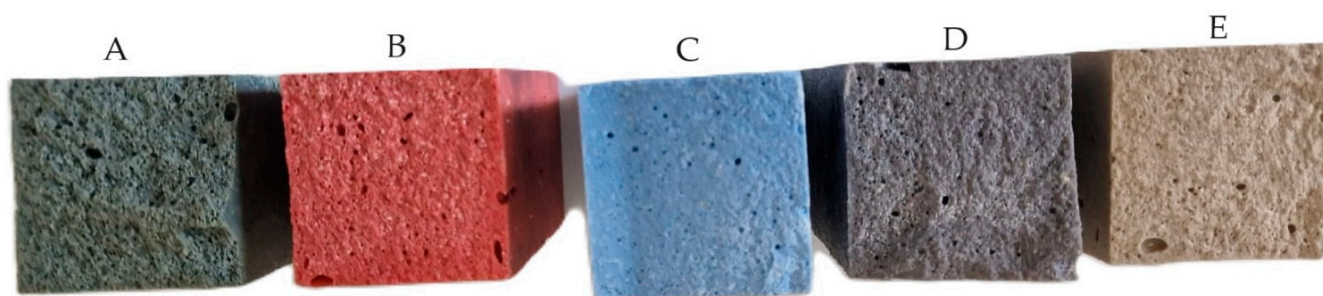

**Figure 6.** Cross-section of five representative samples of epoxy grout, A–E.

3.2.1. SEM Analysis

In Figure 7A,B, the SEM images of Sample A are presented. The magnification of each figure is provided in the respective caption, indicating the degree of enlargement compared

to the actual size of the object. Additionally, the photo scale is depicted in the figures, representing the accuracy of the object's size representation in the image.
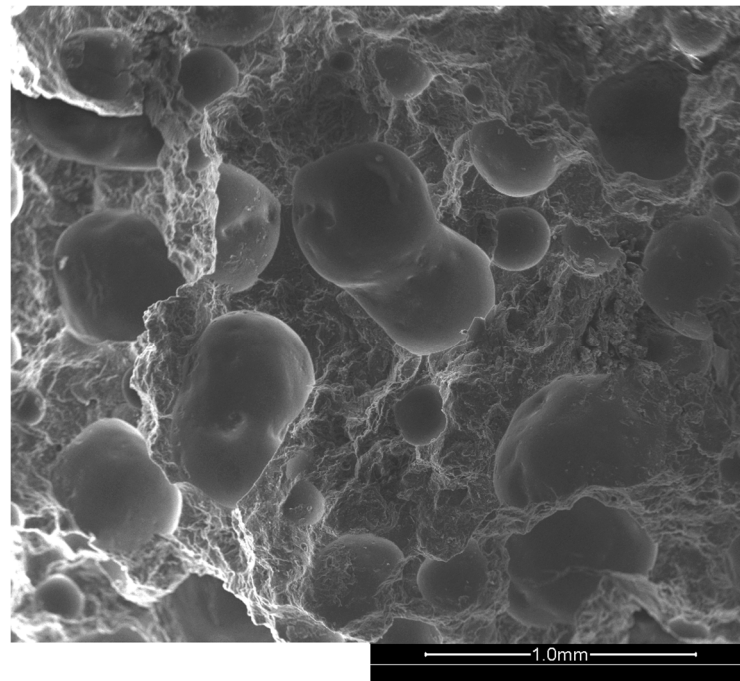

(**A**)
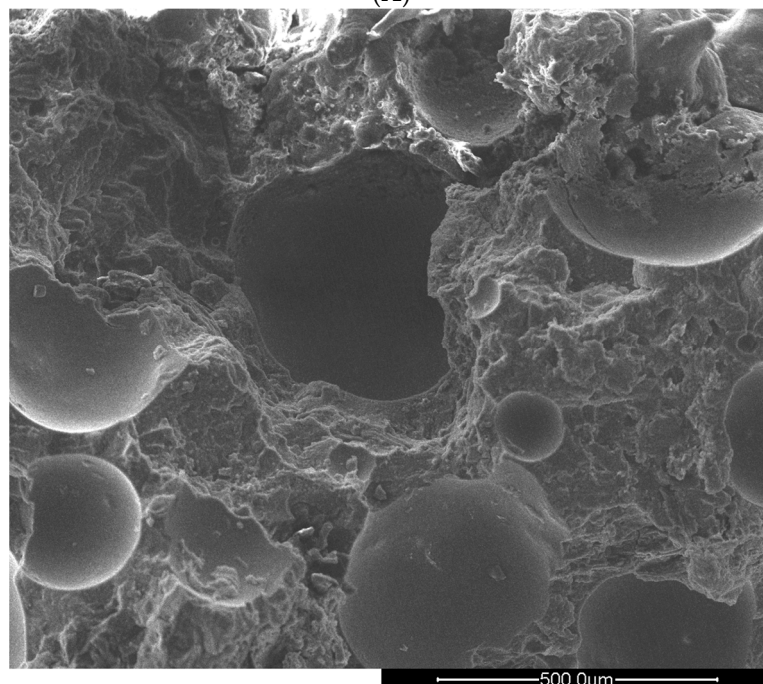
(**B**)

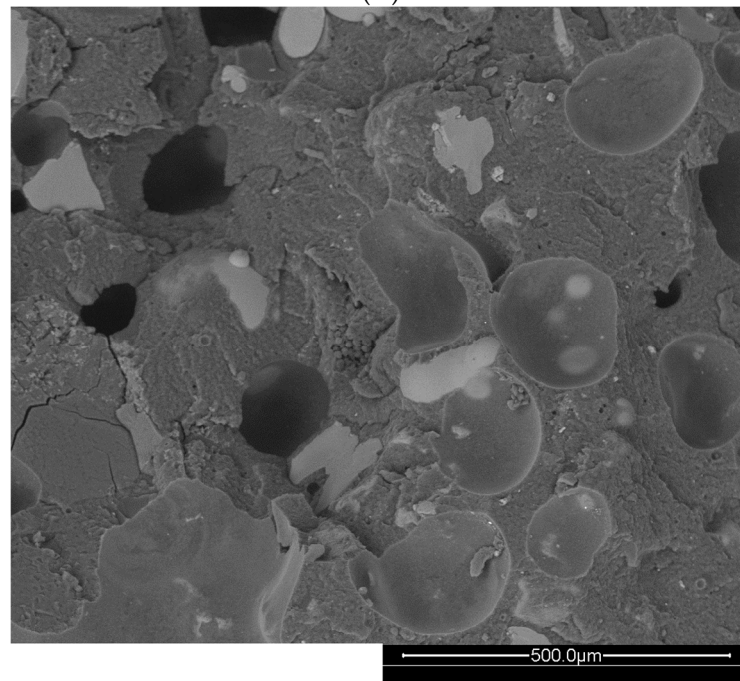**Figure 7.** (**A**) Sample A at 100× magnification. (**B**) Sample A at 200× magnification.

The microstructure exhibits irregularities characterized by numerous cavities. The pseudo-spheroidal olive pit granules are visible, coated within the epoxy resin matrix, and partially embedded. Porosity can be attributed to several factors. Air entrapment during the mixing phase, which is emphasized by the low density of OPP, facilitates this phenomenon. Additionally, the irregular shape of OPP particles can contribute to imperfect distribution within the epoxy matrix, further enhancing porosity formation. Furthermore,

variability in the particle size and agglomeration tendencies of OPP particles may also play a role in porosity development.

In Figure 8A,B, SEM images of Sample E are presented. In contrast to Sample A, the microstructure of Sample E appears significantly more compact. The quartz powder fragments are observed embedded within the epoxy resin, resulting in a compact structure with reduced porosity and cavities. This denser microstructure suggests a more homogeneous distribution of filler particles. There are several pores, likely resulting from air entrapment during the mixing and sample formation stages.
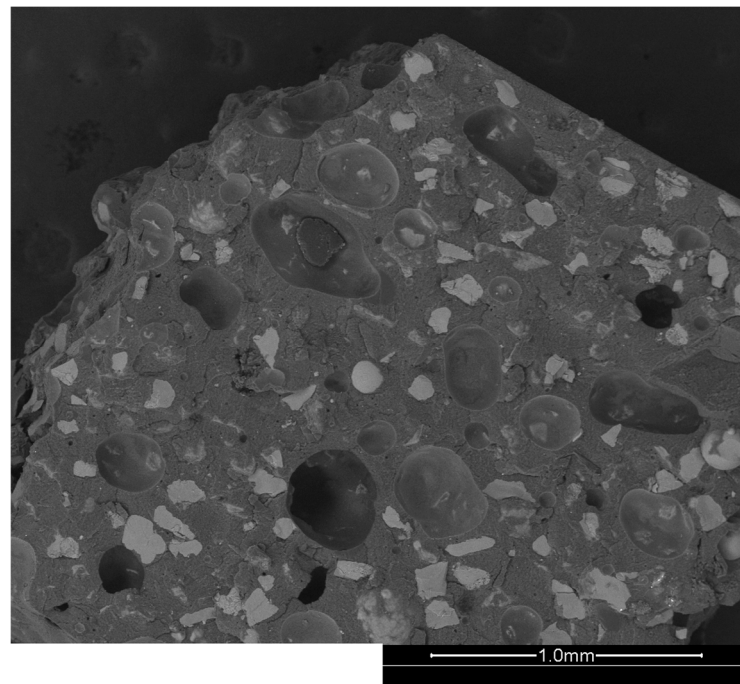
(**A**)

(**B**)

Figure 8. (**A**) Sample E at $100\times$ magnification. (**B**) Sample E at $200\times$ magnification.

3.2.2. Density

The density of epoxy mortars, and more broadly, that of construction materials, is an important parameter that significantly influences various aspects of their performance and applicability. Density plays a key role in determining properties such as thermal and sound insulation, transportation efficiency, and overall environmental impact. The use of materials with lower density in construction contributes to the overall reduction in the weight of structural components, which can be particularly advantageous in applications where weight is a critical factor. Therefore, optimizing and managing the density of construction materials is important to ensure the effectiveness, sustainability, and cost-efficiency of building projects.

The density values of the studied epoxy mortars (A–E) are shown in Figure 9.
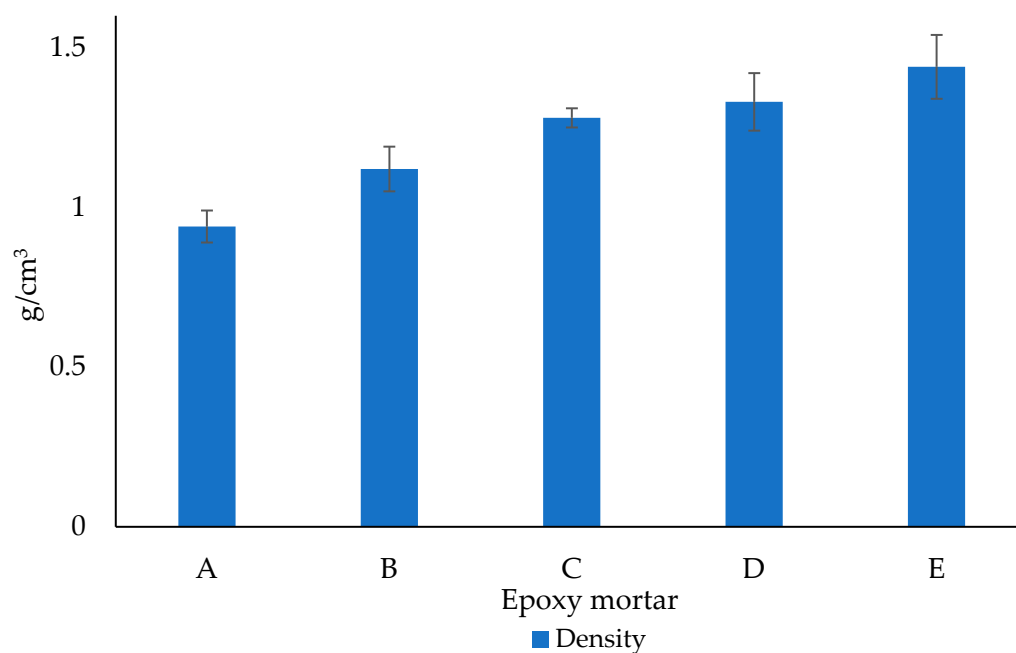
Figure 9. Density of epoxy mortars (A–E) tested after 28 days.

Notably, the bulk density of olive pit powder is considerably lower than that of quartz powder, with values of 0.505 g/cm^3 and 1.7 g/cm^3.

When a higher percentage of olive pit powder is incorporated into the epoxy mortar, a corresponding decrease in the overall density of the mortar is observed. This reduction in density is directly linked to the bulk density of the OPP compared to that of quartz powder. This can also be attributed to the porous structure of the epoxy mortars containing OPP as a filler, which resulted in increased air voids.

3.2.3. Flexural and Compressive Strengths

Flexural and compressive strengths are two crucial mechanical properties used to characterize the behavior of materials under different loading conditions in the field of materials science and engineering. The flexural and compressive strengths of the epoxy mortars (A–E) are shown in Figure 10.

Epoxy mortar A, which contained only OPP as a filler, exhibited the lowest flexural (5.3 MPa) and compressive strengths (12.8 MPa). The introduction of OPP at any level adversely affected both the compressive and flexural strengths. Increases of 64% and 43% were observed in the flexural and compressive strengths, respectively, for Sample B in relation to Sample A. This underscores the substantial improvement in the mechanical properties achieved, even with a minimal addition of quartz powder. Moreover, a more significant decrease in the flexural strength compared to the compressive strength was observed. The data presented in Figure 10 indicate that the inclusion of OPP in epoxy

mortar formulations compromises their suitability for structural applications, as evidenced by the significant reduction in mechanical resistance values.
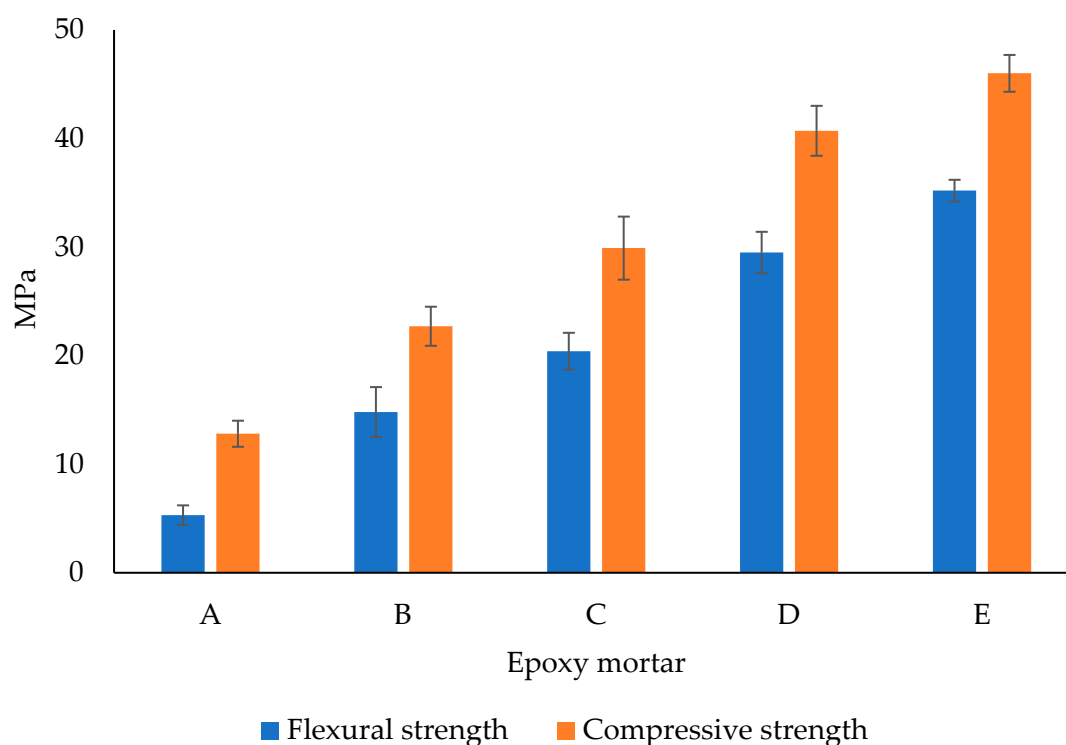
**Figure 10.** Flexural and compressive strengths of epoxy mortars (A–E) tested after 28 days.

As the OPP content increased, the proportion of epoxy resin in the formulation decreased, whereas the reactive diluent content increased, as reported in Table 2. In epoxy grouts containing only inorganic fillers, the proportions of epoxy resin and reactive diluent significantly impact the mechanical properties of the material [45]. A higher concentration of epoxy resin is associated with improved compressive strength, while conversely, a higher concentration of reactive diluent is associated with its decrease. The molecules of reactive diluents become integrated into the network formed after reacting with the hardener. The hardener initiates this reaction by opening the oxirane rings located at the ends of both the epoxy and reactive diluents, thereby bonding the molecules together to establish a network structure. Owing to their aliphatic structures, reactive diluents are smaller and more flexible than rigid epoxy molecules, thus enhancing the flexibility of the epoxy network [45]. Consequently, a decrease in the rigidity of the epoxy backbone may reduce the compressive strength of the material. Moreover, in epoxy grouts containing only inorganic fillers, the addition of diluents generally enhanced the flexural strength of epoxy mortars. This increase is likely attributed to the improved wetting properties of the epoxy–hardener mixture, which may increase the adherence between the mixture and aggregates, and hence the flexural strength. Based on this evidence, we would anticipate that the compressive strength decreases more significantly than the flexural strength when transitioning from specimen E to specimen A. This expectation arises from the decrease in the epoxy resin content and increase in the reactive diluent content. However, the experimental findings presented in Figure 9 reveal the opposite trend. This discrepancy underscores the significant influence of introducing a lignocellulosic material, such as OPP, which substantially modifies the performance of the epoxy mortar. Moreover, it highlights that the presence of OPP has a greater impact on the mechanical properties than variations in resin and reactive thinner content, which exhibit less influence on the final characteristics of the specimens.

The European Standard EN 998-1 [46] specifies requirements for various properties, including compressive strength, for inorganic-binder-based thermal mortars. According to this standard, a compressive strength below 5 MPa is deemed suitable for thermal insulating purposes. With epoxy resin as the binder, our formulations inherently exhibit significantly different properties compared to their inorganic counterparts. Our findings reveal that all tested epoxy-based mortars exceed the compressive strength requirement outlined in the European Standard. Even the lowest compressive strength recorded among our samples is notably higher than the standard's threshold, measuring at 12.8 MPa. This disparity underscores the profound impact of epoxy resin on mortar properties. While inorganic-binder-based mortars may adhere to the standard's compressive strength specifications, epoxy-based alternatives exhibit inherently superior mechanical properties. Our results highlight the need for further evidence or tailored standards to appropriately assess and evaluate the performance of epoxy-based mortars in thermal insulation applications.

3.2.4. Thermal Conductivity

Thermal conductivity is a fundamental property that characterizes the ability of a material to conduct heat. It is defined as the rate at which heat flows through a unit area of a material per unit temperature gradient. This is a critical property in the construction industry, influencing the performance and energy efficiency of buildings and infrastructure. It plays a significant role in controlling heat flow through building materials and assemblies, impacting indoor comfort, energy consumption, and overall building performance. Materials with low thermal conductivity are used as insulation to reduce heat transfer through walls, roofs, floors, and other building components. By minimizing heat flow, thermal insulation helps maintain comfortable indoor temperatures, reduces heating and cooling loads, and lowers energy consumption for heating and air conditioning systems. This is especially important for achieving energy-efficient buildings that comply with energy codes and standards and reduce carbon emissions associated with heating and cooling.

The thermal conductivity data of the studied epoxy mortars (A–E) are shown in Figure 11.
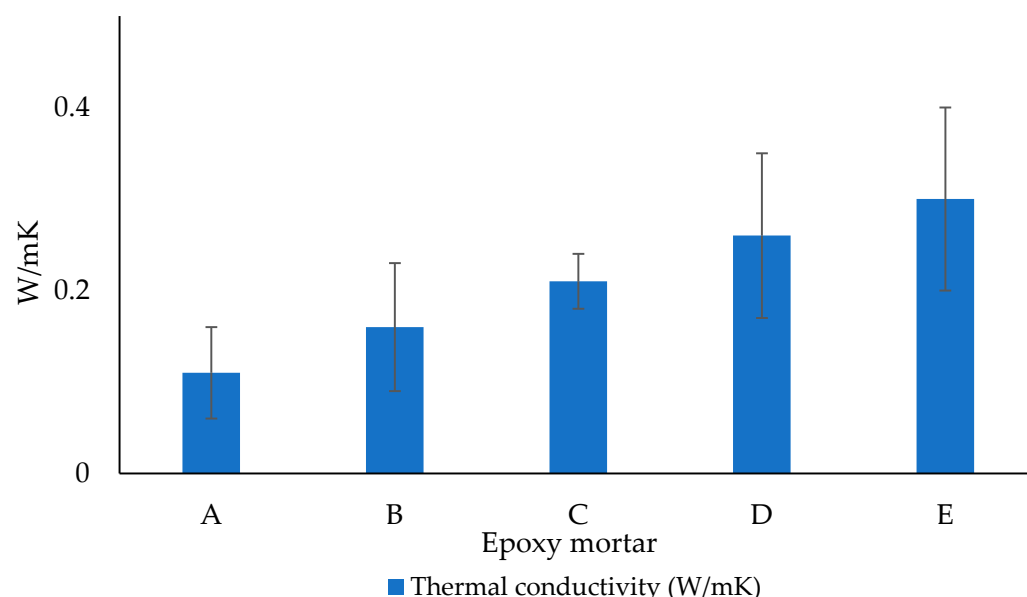
Figure 11. Thermal conductivity (W/mK) of epoxy mortars (A–E) tested after 28 days.

As the proportion of OPP increased in the epoxy mortar formulations, there was a clear trend of decreased thermal conductivity. Epoxy mortar A, predominantly composed of vegetal material, exhibited the lowest thermal conductivity (0.11 W/mK). As the proportion of quartz increased in mortars B through E, there was a corresponding increase in the thermal conductivity. The observed trend can be attributed to the different chemical

composition, as cellulose and lignin have lower thermal conductivities than quartz. Moreover, vegetal materials have a greater capacity to absorb moisture than inorganic materials do. Moisture trapped within a material can act as a thermal insulator, reducing the overall thermal conductivity of the material. Furthermore, as observed from the SEM analysis in Section 3.2.1, Sample A exhibited a microstructure characterized by numerous pores and cavities. This indicates a higher volume of trapped air within the material, resulting in decreased thermal conductivity.

The European Standard EN 998-1 [46] outlines requirements and test methods specifically for inorganic-based thermal insulating mortars [47,48]. According to this document, the mortar thermal conductivity must not exceed 0.2 W/mK. Only OPP_A, OPP_B, and OPP_C mortars appear to meet this criterion. Notably, there is a dearth of evidence regarding epoxy-based mortars containing bio-filler. However, this comparison underscores the potential of epoxy-based mortars with OPP as a filler to meet the thermal insulation standards established for inorganic-based counterparts.

4. Conclusions

In this study, we investigated the potential of olive pit powder (OPP) as a filler in epoxy mortars, aiming to provide insights into its feasibility as a sustainable alternative to traditional inorganic fillers. OPP is considered more sustainable than quartz powder due to its utilization of a waste byproduct from olive oil production, which would otherwise be discarded. This repurposing of waste material aligns with principles of circular economy, minimizing environmental impact and reducing reliance on virgin resources. Additionally, the abundant availability of OPP, particularly in regions with significant olive oil production, further enhances its sustainability profile.

The characterization of olive pit powder (OPP) revealed its lignocellulosic nature and pseudo-spheroidal microstructure, emphasizing its potential as a renewable and environmentally friendly filler material.

Various formulations of epoxy mortar were analyzed, and the OPP and quartz contents were systematically varied. Our findings revealed a consistent trend wherein an increase in the percentage of OPP led to a decrease in density, flexural strength, compressive strength, and thermal conductivity values of the epoxy mortar. This observation can be attributed to several factors, including the lignocellulosic nature of OPP, its inherently low bulk density, and the consequent increase in porosity within the epoxy mortar matrix upon its incorporation. The enhancement of insulating properties and reduction in density, which are crucial factors for thermal efficiency in buildings and energy conservation, are achieved by incorporating OPP into epoxy mortars. However, this improvement comes at the expense of decreased mechanical resistance. Although the data may suggest that epoxy mortar containing OPP is less suitable for structural applications owing to its compromised mechanical resistance, it is important to note that this does not diminish its overall value. The decreased mechanical resistance may limit its use in load-bearing structures; however, it excels in applications where thermal insulation is the primary concern. In these scenarios, the ability of the mortar to effectively minimize heat transfer makes it a highly desirable choice. In addition, its lightweight nature offers advantages in terms of ease of handling and reduced structural load. It is worth mentioning that as our material is novel, there are currently no specific requirements or specifications established for its intended use and applications. Therefore, no direct comparison can be made with the existing literature, and the potential applications of epoxy mortar containing OPP remain to be explored and defined.

Furthermore, our study underscores the importance of considering the synergistic effects of filler properties and content on the overall performance of epoxy mortars. Future research efforts may focus on optimizing the OPP content and exploring additional processing techniques to further enhance the mechanical and thermal properties of epoxy mortars containing OPP.

References

1. Prolongo, S.G.; Del Rosario, G.; Ureña, A. Comparative Study on the Adhesive Properties of Different Epoxy Resins. *Int. J. Adhes. Adhes.* **2006**, *26*, 125–132. [CrossRef]

2. Shamsuddoha, M.; Islam, M.M.; Aravinthan, T.; Manalo, A.; Lau, K. Characterisation of Mechanical and Thermal Properties of Epoxy Grouts for Composite Repair of Steel Pipelines. *Mater. Des. 1980-2015* **2013**, *52*, 315–327. [CrossRef]

3. Wang, W.; Zhao, W.; Zhang, J.; Zhou, J. Epoxy-Based Grouting Materials with Super-Low Viscosities and Improved Toughness. *Constr. Build. Mater.* **2021**, *267*, 121104. [CrossRef]

4. Zhou, Q.; Hao, J.P.; Lv, P.; Men, J.J. Study on a New Adhesive of Concrete Cracks Repairing. *Adv. Mater. Res.* **2010**, *168–170*, 1308–1312.

5. Anagnostopoulos, C.A. Laboratory Study of an Injected Granular Soil with Polymer Grouts. *Tunn. Undergr. Space Technol.* **2005**, *20*, 525–533. [CrossRef]

6. Yemam, D.M.; Kim, B.-J.; Moon, J.-Y.; Yi, C. Mechanical Properties of Epoxy Resin Mortar with Sand Washing Waste as Filler. *Materials* **2017**, *10*, 246. [CrossRef]

7. Lakhiar, M.T.; Bai, Y.; Wong, L.S.; Paul, S.C.; Anggraini, V.; Kong, S.Y. Mechanical and Durability Properties of Epoxy Mortar Incorporating Coal Bottom Ash as Filler. *Constr. Build. Mater.* **2022**, *315*, 125677. [CrossRef]

8. Dębska, B.; Lichołai, L. The Selected Mechanical Properties of Epoxy Mortar Containing PET Waste. *Constr. Build. Mater.* **2015**, *94*, 579–588. [CrossRef]

9. Pacheco-Torgal, F.; Shasavandi, A.; Jalali, S. Eco-Efficient Concrete Using Industrial Wastes: A Review. *Mater. Sci. Forum* **2012**, *730–732*, 581–586.

10. Zhang, S.; Shinwari, R.; Zhao, S.; Dagestani, A.A. Energy Transition, Geopolitical Risk, and Natural Resources Extraction: A Novel Perspective of Energy Transition and Resources Extraction. *Resour. Policy* **2023**, *83*, 103608. [CrossRef]

11. Sun, Y.; Li, Y.; Yu, T.; Zhang, X.; Liu, L.; Zhang, P. Resource Extraction, Environmental Pollution and Economic Development: Evidence from Prefecture-Level Cities in China. *Resour. Policy* **2021**, *74*, 102330. [CrossRef]

12. Bărbuţă, M.; Harja, M.; Baran, I. Comparison of Mechanical Properties for Polymer Concrete with Different Types of Filler. *J. Mater. Civ. Eng.* **2009**, *22*, 696–701. [CrossRef]

13. Reis, J.M.L. Fracture and Flexural Assessment of Red Mud in Epoxy Polymer Mortars. *Mater. Struct.* **2015**, *48*, 3929–3936. [CrossRef]

14. Singh, G.; Kumar, H.; Singh, S. Performance Evaluation-PET Resin Composite Composed of Red Mud, Fly Ash and Silica Fume. *Constr. Build. Mater.* **2019**, *214*, 527–538. [CrossRef]

15. Onaizi, A.M.; Tang, W.; Amran, M.; Liu, Y.; Sajjad, U.; Alhassan, M. Towards Increased Adoption of Furnace Bottom Ash as Sustainable Building Materials: Characterization, Standardization, and Applications. *J. Build. Eng.* **2024**, *82*, 108274. [CrossRef]

16. Lokuge, W.; Aravinthan, T. Effect of Fly Ash on the Behaviour of Polymer Concrete with Different Types of Resin. *Mater. Des.* **2013**, *51*, 175–181. [CrossRef]

17. Yeon, J. Deformability of Bisphenol A-Type Epoxy Resin-Based Polymer Concrete with Different Hardeners and Fillers. *Appl. Sci.* **2020**, *10*, 1336. [CrossRef]

18. Khalid, N.H.A.; Hussin, M.W.; Mirza, J.; Ariffin, N.F.; Ismail, M.A.; Lee, H.-S.; Mohamed, A.; Jaya, R.P. Palm Oil Fuel Ash as Potential Green Micro-Filler in Polymer Concrete. *Constr. Build. Mater.* **2016**, *102*, 950–960. [CrossRef]

19. D'Eusanio, V.; Bertacchini, L.; Marchetti, A.; Mariani, M.; Pastorelli, S.; Silvestri, M.; Tassi, L. Rosaceae Nut-Shells as Sustainable Aggregate for Potential Use in Non-Structural Lightweight Concrete. *Waste* **2023**, *1*, 549–568. [CrossRef]

20. Wu, F.; Yu, Q.; Liu, C. Durability of Thermal Insulating Bio-Based Lightweight Concrete: Understanding of Heat Treatment on Bio-Aggregates. *Constr. Build. Mater.* **2021**, *269*, 121800. [CrossRef]

21. Qiao, Y.; Li, Q.; Li, Q.; Yang, K.; Bai, C.; Zhang, L.; Yao, Z.; Wang, P.; Zheng, T.; Zhang, X.; et al. Improving Thermal Insulation Properties of Lightweight Epoxy Resin Matrix Composites with Millimeter-Sized Hollow Glass Microspheres/Epoxy Hollow Spheres. *Energy Build.* **2022**, *277*, 112546. [CrossRef]

22. Aditya, L.; Mahlia, T.M.I.; Rismanchi, B.; Ng, H.M.; Hasan, M.H.; Metselaar, H.S.C.; Muraza, O.; Aditiya, H.B. A Review on Insulation Materials for Energy Conservation in Buildings. *Renew. Sustain. Energy Rev.* **2017**, *73*, 1352–1365. [CrossRef]

23. Kumar, D.; Alam, M.; Zou, P.X.W.; Sanjayan, J.G.; Memon, R.A. Comparative Analysis of Building Insulation Material Properties and Performance. *Renew. Sustain. Energy Rev.* **2020**, *131*, 110038. [CrossRef]

24. Jelle, B.P. Traditional, State-of-the-Art and Future Thermal Building Insulation Materials and Solutions—Properties, Requirements and Possibilities. *Energy Build.* **2011**, *43*, 2549–2563. [CrossRef]

25. Xu, X.; Zhang, Y.; Lin, K.; Di, H.; Yang, R. Modeling and Simulation on the Thermal Performance of Shape-Stabilized Phase Change Material Floor Used in Passive Solar Buildings. *Energy Build.* **2005**, *37*, 1084–1091. [CrossRef]

26. Hammid, A.T.; Jebur, Y.M.; Lafta, H.A.; Parwata, I.W.; Patra, I.; Arenas, L.A.B. The Arrangement of Phase Change Materials inside a Building Wall and Its Energy Performance. *Sustain. Energy Technol. Assess.* **2023**, *57*, 103158. [CrossRef]

27. Bergmann Becker, P.F.; Effting, C.; Schackow, A. Lightweight Thermal Insulating Coating Mortars with Aerogel, EPS, and Vermiculite for Energy Conservation in Buildings. *Cem. Concr. Compos.* **2022**, *125*, 104283. [CrossRef]

28. *EN 13888-1:2022*; Grouts for Ceramic Tiles—Requirements Evaluation of Conformity, Classification and Designation. European Committee for Standardization: Brussels, Belgium, 2022.

29. *ISO 13007*; Ceramic Tiles, Grouts and Adhesives; Part 3: Terms, Definitions and Specifications for Grouts. International Organization for Standardization: Geneva, Switzerland, 2010.

30. *ASTM D5334-08*; Standard Test Method for Determination of Thermal Conductivity of Soil and Soft Rock by Thermal Needle Probe Procedure. ASTM International: West Conshohocken, PA, USA, 2014.

31. D'Eusanio, V.; Morelli, L.; Marchetti, A.; Tassi, L. Aroma Profile of Grapevine Chips after Roasting: A Comparative Study of Sorbara and Spergola Cultivars for More Sustainable Oenological Production. *Separations* **2023**, *10*, 532. [CrossRef]

32. Sonwani, E.; Bansal, U.; Alroobaea, R.; Baqasah, A.M.; Hedabou, M. An Artificial Intelligence Approach Toward Food Spoilage Detection and Analysis. *Front. Public Health* **2022**, *9*, 816226. [CrossRef]

33. D'Eusanio, V.; Malferrari, D.; Marchetti, A.; Roncaglia, F.; Tassi, L. Waste By-Product of Grape Seed Oil Production: Chemical Characterization for Use as a Food and Feed Supplement. *Life* **2023**, *13*, 326. [CrossRef]

34. D'Eusanio, V.; Genua, F.; Marchetti, A.; Morelli, L.; Tassi, L. Exploring the Mineral Composition of Grapevine Canes for Wood Chip Applications in Alcoholic Beverage Production to Enhance Viticulture Sustainability. *Beverages* **2023**, *9*, 60. [CrossRef]

35. Abdullah, S.; Suzana, Y.; Ahmad, M.; Ramli, A.; Ismail, L. Thermogravimetry Study on Pyrolysis of Various Lignocellulosic Biomass for Potential Hydrogen Production. *Int. J. Chem. Biol. Eng.* **2010**, *3*, 750–754.

36. Şen, D.; Gökmen, V. Kinetic Modeling of Maillard and Caramelization Reactions in Sucrose-Rich and Low Moisture Foods Applied for Roasted Nuts and Seeds. *Food Chem.* **2022**, *395*, 133583. [CrossRef] [PubMed]

37. Weiss, I.M.; Muth, C.; Drumm, R.; Kirchner, H.O.K. Thermal Decomposition of the Amino Acids Glycine, Cysteine, Aspartic Acid, Asparagine, Glutamic Acid, Glutamine, Arginine and Histidine. *BMC Biophys.* **2018**, *11*, 2. [CrossRef] [PubMed]

38. Shen, D.K.; Gu, S. The Mechanism for Thermal Decomposition of Cellulose and Its Main Products. *Bioresour. Technol.* **2009**, *100*, 6496–6504. [CrossRef] [PubMed]

39. González Martínez, M.; Anca Couce, A.; Dupont, C.; da Silva Perez, D.; Thiéry, S.; Meyer, X.; Gourdon, C. Torrefaction of Cellulose, Hemicelluloses and Lignin Extracted from Woody and Agricultural Biomass in TGA-GC/MS: Linking Production Profiles of Volatile Species to Biomass Type and Macromolecular Composition. *Ind. Crops Prod.* **2022**, *176*, 114350. [CrossRef]

40. Shapiro, A.J.; O'Dea, R.M.; Epps, T.H.I. Thermogravimetric Analysis as a High-Throughput Lignocellulosic Biomass Characterization Method. *ACS Sustain. Chem. Eng.* **2023**, *11*, 17216–17223. [CrossRef]

41. Song, C.; Hu, H.; Zhu, S.; Wang, G.; Chen, G. Nonisothermal Catalytic Liquefaction of Corn Stalk in Subcritical and Supercritical Water. *Energy Fuels* **2004**, *18*, 90–96. [CrossRef]

42. Carrier, M.; Loppinet-Serani, A.; Denux, D.; Lasnier, J.-M.; Ham-Pichavant, F.; Cansell, F.; Aymonier, C. Thermogravimetric Analysis as a New Method to Determine the Lignocellulosic Composition of Biomass. *Biomass Bioenergy* **2011**, *35*, 298–307. [CrossRef]

43. Zhao, C.; Jiang, E.; Chen, A. Volatile Production from Pyrolysis of Cellulose, Hemicellulose and Lignin. *J. Energy Inst.* **2017**, *90*, 902–913. [CrossRef]

44. Yeo, J.Y.; Chin, B.L.F.; Tan, J.K.; Loh, Y.S. Comparative Studies on the Pyrolysis of Cellulose, Hemicellulose, and Lignin Based on Combined Kinetics. *J. Energy Inst.* **2019**, *92*, 27–37. [CrossRef]

45. Ozeren Ozgul, E.; Ozkul, M.H. Effects of Epoxy, Hardener, and Diluent Types on the Hardened State Properties of Epoxy Mortars. *Constr. Build. Mater.* **2018**, *187*, 360–370. [CrossRef]

46. *EN 998-1*; Specification for Mortar for Masonry—Part 1: Rendering and Plastering Mortar. European Committee for Standardization: Brussels, Belgium, 2018.

47. Parracha, J.L.; Santos, A.R.; Lazera, R.; Flores-Colen, I.; Gomes, M.G.; Rodrigues, A.M. Performance of Lightweight Thermal Insulating Mortars Applied on Brick Substrate Specimens and Prototype Wall. *Constr. Build. Mater.* **2023**, *364*, 129954. [CrossRef]
48. Soares, A.; De Fátima Júlio, M.; Flores-Colen, I.; Ilharco, L.M.; Brito, J.D. EN 998-1 Performance Requirements for Thermal Aerogel-Based Renders. *Constr. Build. Mater.* **2018**, *179*, 453–460. [CrossRef]